Steady State Kinetics of Spleen Tyrosine Kinase Investigated by a Real Time Fluorescence Assay

Eva Papp,[‡] Joyce K. Y. Tse,[‡] Hoangdung Ho,[§] Sandra Wang,[§] David Shaw,[§] Simon Lee,[§] Jim Barnett,[§] David C. Swinney,[‡] and J. Michael Bradshaw*,[‡]

Departments of Biochemical Pharmacology and Molecular and Protein Sciences, Roche Palo Alto LLC, 3431 Hillview Avenue, Palo Alto, California 94304

Received August 8, 2007; Revised Manuscript Received September 22, 2007

ABSTRACT: Spleen tyrosine kinase (Syk) is a cytoplasmic tyrosine kinase that plays an important signaling role in several types of immune cells. To improve our understanding of the enzymology and activation mechanism of Syk, we characterized the steady state kinetics of Syk substrate phosphorylation. A new real time fluorescence kinase assay was employed that utilizes a nonnatural amino acid in the peptide substrate which undergoes an enhancement in fluorescence following phosphorylation. Characterizing the steady state kinetics using a Syk kinase domain construct [Syk(360−635)] revealed that Syk employs a ternary complex kinetic mechanism involving little cooperativity between substrate binding sites and a K_m(ATP) of 36 ± 5 μM and a K_m(peptide substrate) of 4.4 ± 0.9 μM. The order of substrate binding was determined to be either random or ordered with ATP binding first, as determined in substrate analogue inhibitor studies. Utilizing the real time capabilities of the fluorescence assay, we established that Syk demonstrates no lag phase in product formation. Furthermore, a Syk mutant lacking tyrosine in the activation loop (Syk Y525F,Y526F) exhibited activity identical to that of wild-type Syk. These two findings indicate that autophosphorylation of the activation loop of Syk does not regulate Syk(360−635) activity. We also compared the activity of Syk(360−635) to that of full-length Syk and revealed that Syk(360−635) is 10-fold more active, suggesting that residues outside the catalytic domain of Syk suppress kinase activity. The findings presented here provide the first kinetic description of the Syk enzyme mechanism.

Spleen tyrosine kinase (Syk)[1] is a widely expressed nonreceptor tyrosine kinase that facilitates signal transduction in diverse cell types (*1*−*4*). Syk plays a particularly important role in B cells, mast cells, and macrophages (*5*−*7*). The significance of Syk in B cells was first deduced from Syk knockout mice (*8*). These mice die perinatally, and syk$^{-/-}$ lymphoid cells are impaired in B cell maturation due to ablated signaling downstream of the B cell receptor. In mast cells, Syk has been shown to be required for degranulation in response to FcϵRI receptor aggregation (*9, 10*). The central role of Syk in hematopoietic cells such as B cells and mast cells makes Syk an attractive target for diseases such as rheumatoid arthritis, asthma, and allergic rhinitis (*11, 12*).

The molecular events involving Syk that couple receptor ligation to signal propagation have been well established (*13, 14*). Syk is located downstream of the B cell receptor in B cells, FcϵRI receptor in mast cells, and Fc$R\gamma$ receptor in macrophages. Signaling is initiated in each cell type with extracellular ligation of the receptor, which first causes activation of Src family tyrosine kinases in the intracellular compartment. Src family kinases proceed to phosphorylate the cytoplasmic tail of the receptor within immune tyrosine activation motifs (ITAMs), which are two YxxL sequences typically spaced 7−12 residues apart. Following ITAM phosphorylation, Syk is recruited to the plasma membrane by binding to these phosphorylated ITAM sequences. Syk itself then becomes phosphorylated by Src family kinases. Syk subsequently phosphorylates downstream targets such as BLNK in B cells and PKCα in mast cells, resulting in further propagation of the signal.

The Syk protein structure consists of an N-terminal tandem set of SH2 domains, a linker region, and a C-terminal kinase domain (see Figure 1A). Each domain has a particular function: the tandem SH2 domains facilitate binding to ITAM sequences (*15*−*17*), the linker region serves as a region of regulatory phosphorylation and protein docking (*18*−*20*), and the kinase domain phosphorylates cellular substrates (*5*−*7*). Syk has been shown to undergo alternative splicing. Specifically, a variant of Syk known as SykB lacks 23 amino acids within the linker region; SykB is less capable than Syk in facilitating immune cell signaling processes (*21*). Syk has the same overall domain structure as its close homologue Zap-70 which plays a role in signaling in T cells analogous to that of Syk in B cells (*22*).

Several questions regarding the molecular mechanism of Syk remain uncharacterized. Syk has yet to be studied using

* To whom correspondence should be addressed. Telephone: (650) 855-5592. Fax: (650) 855-6078. E-mail: Michael.bradshaw@roche.com.
[‡] Department of Biochemical Pharmacology.
[§] Department of Molecular and Protein Sciences.

[1] Abbreviations: Syk, spleen tyrosine kinase; ITAM, immune tyrosine activation motif; SH2, Src homology 2; BLNK, B cell linker protein; PKCα, protein kinase Cα; Zap-70, zeta chain-associated protein kinase 70; Csk, C-terminal Src kinase; Btk, Bruton's tyrosine kinase; DTT, dithiothreitol; BSA, bovine serum albumin; Aca, 4-aminocyclohexylalanine.

10.1021/bi701596u CCC: $37.00
Published on Web 12/01/2007

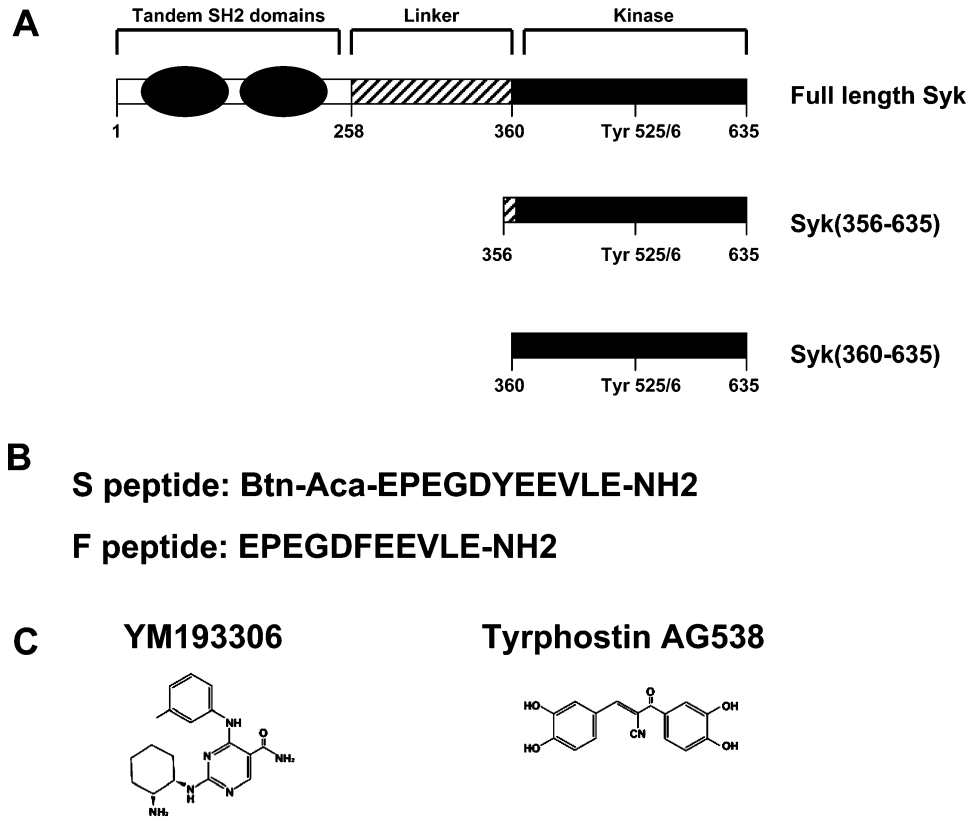

FIGURE 1: Sequences and structures of the proteins, substrates, and inhibitors used in this study. (A) Domain structure of Syk and Syk constructs used in this study. Full-length Syk contains an N-terminal tandem set of SH2 domains, a linker region, and a C-terminal kinase domain. Two constructs used in this study, Syk(356−635) and Syk(360−635), consist of just the kinase domain. (B) Peptide sequences for the S peptide and F peptide. Amino acids are listed by single-letter code except for those of biotin (Btn) and 4-aminocyclohexylalanine (Aca), which was used as an amino acid linker between biotin and the peptide. Peptides were synthesized using standard Fmoc chemistry. (C) Chemical structures for YM193306 and tyrphostin AG538 (Calbiochem, San Diego, CA).

steady state kinetics to elucidate the kinetic constants and order of substrate binding. Furthermore, while a few experiments have explored the significance of activation loop phosphorylation within cells (*23*, *24*), no study has yet quantitatively addressed how activation loop phosphorylation affects Syk activity in vitro. Finally, while evidence suggests that both ITAM binding and phosphorylation outside the activation loop play a role in Syk activation (*25*−*27*), a clear picture of how Syk becomes activated following receptor activation has not yet emerged.

In this study, we have used a new real time fluorescence assay to examine the enzymology and activation mechanism of Syk. Comparison of this fluorescence assay with an end point radioactive kinase assay revealed that the different methodologies provided similar information. We found evidence that Syk forms a ternary complex with its two substrates. Furthermore, several lines of evidence pointed to there being little role for activation loop autophosphorylation in regulating the activity of the Syk kinase domain. Finally, comparison of the activity of full-length Syk with that of a kinase-only truncated version of Syk revealed a 10-fold greater activity of the truncated version, suggesting a negative regulatory role for the tandem SH2 domains and linker region of Syk. These studies provide the first detailed kinetic characterization of Syk and may be useful for devising strategies for targeting Syk for treatment of disorders of the immune system.

RESULTS

A Direct, Real Time Fluorescence Assay for Monitoring Syk Activity Using the Sox Fluorophore. Recently, a novel approach to directly monitoring the activity of protein kinases using real time fluorescence has been developed (*28*, *29*). This technique utilizes an unnatural, fluorescent amino acid, the Sox amino acid, incorporated into the substrate peptide of interest. Placing the Sox amino acid appropriately within the peptide results in an increase in the fluorescence intensity of Sox following phosphorylation due to more efficient coordination of Mg^{2+} (see Figure 2). Using the Sox fluorophore, the activity of protein kinases can be directly evaluated in real time using a simple fluorescent readout.

We set out to examine if a Sox-based kinase assay had utility for performing detailed kinetic and mechanistic studies with protein kinases. If so, we planned to use the Sox-based method together with a radioactive kinase assay to perform a kinetic characterization of the Syk tyrosine kinase. We first noted that several commercially available Sox-containing peptides (termed pep 3, pep 5, and pep 7) are reported to be capable of serving as Syk substrates (see Experimental Procedures). To identify which of these peptides might be optimal for a kinetic characterization of Syk, each peptide was incubated together with Syk and Mg^{2+}/ATP and the change in fluorescence intensity was monitored. In these initial experiments, a truncated version of Syk consisting of only its kinase domain, Syk(360−635), was used (Figure 1A). The Syk(360−635) construct had the highest activity

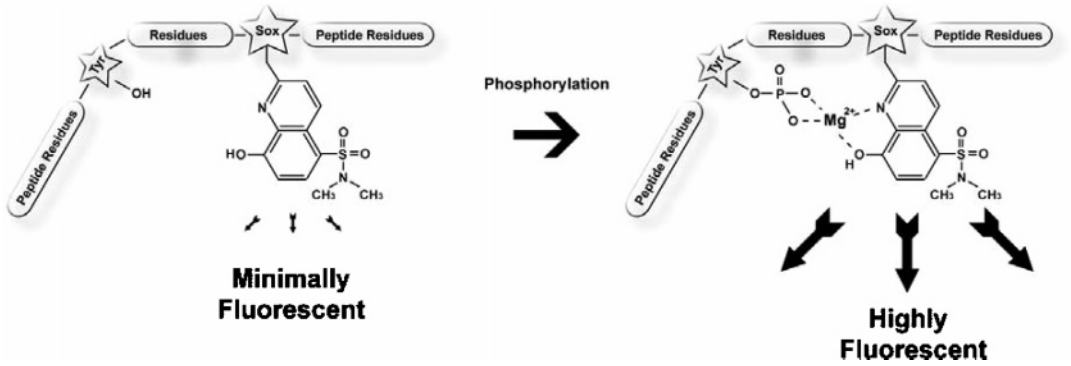

FIGURE 2: Molecular basis for a real time kinase assay using a Sox-containing peptide. In the absence of phosphorylation, the Sox-containing peptide is minimally fluorescent (left panel). However, following phosphorylation, the Sox amino acid more strongly binds Mg^{2+} (right panel), causing a significant increase in the fluorescence intensity of the Sox fluorophore.

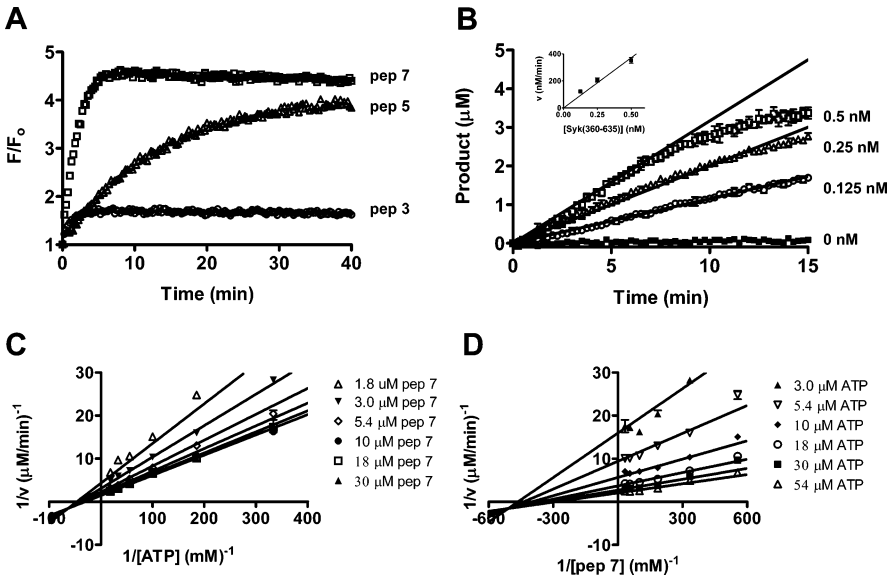

FIGURE 3: Activity of Syk monitored using a real time fluorescence kinase assay. (A) The rate of product formation and the magnitude of signal change depend on the Sox-containing peptide. Three peptides (pep 3, pep 5, and pep 7) were explored as Syk substrates at a Syk(360−635) concentration of 10 nM. Shown is the increase in peptide fluorescence following phosphorylation (F/F_o) as a function of time (minutes). Pep 3, pep 5, and pep 7 demonstrated 1.7-, 4.0-, and 4.5-fold total increases in fluorescence as well as activities of 1.8, 0.2, and 2.5 fluorescence units/min, respectively. Hence, pep 7 demonstrated the greatest signal change and most rapid conversion of substrate to product. (B) Activity of Syk(360−635) at different Syk(360−635) concentrations using pep 7 as a substrate. Shown is the time course of product formation as a function of time at 0, 0.125, 0.25, and 0.5 nM Syk(360−635). The solid lines are the linear best fits to the initial phase of the reaction time courses (10 min for 0.125 and 0.25 nM Syk, 5 min for 0.5 nM Syk). The inset shows the velocity as a function of Syk(360−635) concentration. In this plot, the solid line is the linear best fit to the data, the slope of which provides a turnover rate of 726 ± 39 min^{-1} for these experiments. (C and D) Two-substrate kinetic analysis using a real time fluorescence assay demonstrates that Syk employs a sequential, or ternary complex, kinetic mechanism. Shown are double-reciprocal plots of $1/v$ vs 1/[ATP] (C) and $1/v$ vs 1/[pep 7] (D). Solid lines are simulations based on the parameters in Table 1 derived from the nonlinear least-squares best fit of the entire data set to the ternary complex kinetic model (eq 2). See Figure 2 of the Supporting Information for a representation of the data in Michaelis−Menten form. Error bars are the standard deviations of multiple data points under each condition.

of several examined Syk constructs in a preliminary evaluation of Syk activity (data not shown). Figure 3A shows that pep 5 and pep 7 both exhibit a large increase in fluorescence intensity upon incubation with Syk(360−635) while the change in the fluorescence of pep 3 was much smaller. However, the increase in the fluorescence of pep 7 was more rapid than that of either pep 5 or pep 3. On the basis of this experiment, pep 7 was chosen as the primary Sox-based substrate for the kinetic characterization of Syk.

To confirm that the change in fluorescence reflects specific phosphorylation of the peptide by Syk(360−635), the change in fluorescence of pep 7 with time was examined as a function of enzyme concentration. The kinetic traces are shown in Figure 3B. Omitting Syk from the reaction was first observed to result in no change in fluorescence with time (Figure 3B). At all other enzyme concentrations, the extent of product formation was found to increase linearly with time until at least 20% or more of the substrate was depleted (Figure 3B). The enzyme concentration dependence of the velocity (see the Figure 3B inset) was linear at the low concentrations of Syk(360−635) employed in this experiment. These findings are all consistent with catalytic conversion of pep 7 to its phosphorylated form by Syk(360−635), providing validation that the observed fluorescence signal reflects specific phosphorylation of the substrate. To further validate that the change in fluorescence resulted from specific peptide phosphorylation by Syk, the enzyme concentration dependence of pep 5 phosphorylation was also studied (see Figure 1A of the Supporting Information). Experiments using pep 5 instead of pep 7 gave qualitatively

Table 1: Kinetic Constants from the Two-Substrate Kinetic Analysis[a]

assay	substrate	K_m (μM)	K_a (μM)	V_{max} (μM/min)	k_{cat} (min^{-1})	α
fluorescence	ATP	36 ± 5	16 ± 7	0.80 ± 0.06	1600 ± 120	2.2 ± 0.9
fluorescence	pep 7	4.4 ± 0.9	2.0 ± 0.7	0.80 ± 0.06	1600 ± 120	2.2 ± 0.9
radioactive	ATP	23 ± 5	20 ± 11	0.19 ± 0.01	380 ± 20	1.1 ± 0.7
radioactive	S peptide	8.4 ± 2	7.4 ± 4	0.19 ± 0.01	380 ± 20	1.1 ± 0.7

[a] Parameters are derived from the global, nonlinear best fit of the velocity data to the ternary complex model (eq 2). Uncertainties represent the standard error for each parameter from the global fitting procedure.

the same results, although the velocity of the reaction was slower.

Two-Substrate Kinetic Analysis: Comparison of the Real Time Fluorescence Assay to a Radioactive Enzyme Assay. The results described above suggest that the observed fluorescence signal of the Sox-based assay accurately reflects substrate phosphorylation by Syk. Since the methodology is new, we decided to further validate the approach by directly comparing results from the fluorescence assay to those obtained using an end point radioactive kinase assay. A radioactive assay for Syk activity was developed on the basis of the capture of a biotinylated substrate peptide using streptavidin-coated beads (see Experimental Procedures). For the radioactive assay, reaction conditions were optimized such that product formation was linear with time for at least 20 min and the velocity of the reaction was linear with enzyme concentration (Figure 1B of the Supporting Information).

The real time fluorescence assay and the radioactive assay were both used to perform a two-substrate kinetic analysis of Syk(360−635) in which the reaction velocity was measured as a function of both ATP concentration and peptide substrate concentration. These experiments sought to determine (1) K_m values for both ATP and the peptide substrate, (2) whether the reaction occurred via a ternary complex of Syk(360−635), ATP, and peptide substrate, and (3) the communication between the two substrate binding sites. The results are shown in panels C and D of Figure 3 and also in Figure 2 of the Supporting Information.

Results using both methods were analyzed in an identical manner. The entire data sets were simultaneously fit to either a ternary complex (see eq 2) or ping-pong (see eq 4) reaction mechanism. The ternary complex model provided the better fit in both cases, which was expected on the basis of the intersecting line pattern in the double-reciprocal plots (Figure 3 and Figure 2 of the Supporting Information). The best fit parameters for the fluorescence experiments (Table 1) indicate that the K_m for ATP was 36 ± 5 μM and the K_m for pep 7 was 4.4 ± 0.9 μM. The α factor, a measure of the communication between the ATP and peptide binding sites (*30*, *31*), was 2.2 ± 0.9, indicating that ATP binding has little effect on pep 7 binding and vice versa. The radioactive capture method provided K_m values and α factor values for Syk(360−635) similar to those of the real time fluorescence method (Table 1). The maximum velocities were different for the two approaches: V_{max}(fluorescence) = 0.8 ± 0.06 μM/min (or k_{cat} = 1600 min^{-1}) versus V_{max}(radioactive) = 0.19 ± 0.01 μM/min (or k_{cat} = 380 min^{-1}). This is likely due to the different peptide substrates employed using the fluorescence (pep 7) and radioactive (S pep) methods. Other than V_{max}, the fluorescence assay appeared to provide information similar to that of the radioactive assay, further validating the applicability of the real time fluorescence approach for studying the Syk enzyme mechanism.

Role of Activation Loop Phosphorylation in Syk Kinase Domain Activity. We proceeded to use the real time fluorescence assay to explore whether phosphorylation of tyrosines within the activation loop of the Syk kinase domain modulates its activity. Phosphorylation in the activation loop is essential for maximal activity for many kinases, and Syk has two activation loop tyrosines (Tyr 525 and Tyr 526) that could be hypothesized to regulate catalysis. However, comparison of the activity of the wild-type Syk kinase domain with a Syk Y525F,Y526F mutant revealed no significant difference in activity (Figure 4A), suggesting that phosphorylation of Tyr 525 and Tyr 526 plays no role in activating the Syk kinase domain. This finding reinforces a previous observation that little to no initial lag phase occurs in the Syk kinase domain reaction time course (see Figure 3B), which also suggested that the kinase domain is already in its fully activated state prior to inclusion of substrate and Mg^{2+}/ATP. In addition to using the fluorescence assay to examine the activity of Syk Y525F,Y526F, we also used the radioactive assay; identical time courses for the wild type and mutant were also observed using this method (see Figure 1C of the Supporting Information).

To further explore the potential role of activation loop phosphorylation in regulating Syk kinase domain activity, we probed the phosphorylation state of the activation loop using Western blotting with a Tyr 525/526 phosphospecific antibody. It was observed that the Syk kinase domain is moderately phosphorylated in its activation loop in its purified, basal state (Figure 4B). Incubation with 100 μM ATP increases the level of activation loop phosphorylation, while treatment with tyrosine phosphatase PTP1B eliminates phosphorylation (Figure 4B). The kinetics of the basal, preincubated, and dephosphorylated forms of the Syk kinase domain were compared, and equivalent values of the kinetic constants were observed for each form the protein (Figure 4C,D and Table 2). This finding supports the notion that activation loop phosphorylation does not regulate the activity of the Syk kinase domain.

Order of Substrate Binding Investigated Using Substrate Analogue Inhibitors. We next investigated the order of substrate binding to Syk by exploring the mechanism of inhibition (competitive, noncompetitive, or uncompetitive) of substrate analogue inhibitors. The radioactive kinase assay was employed in these experiments since it was more cost-effective due to the high substrate concentrations that are required.

The first experiments focused on the ATP binding site using the known Syk inhibitor YM193306 (*32*, *33*; see Figure 1C). The concentration of YM193306 was varied from 0.5 to 50 nM while simultaneously either ATP or S peptide was

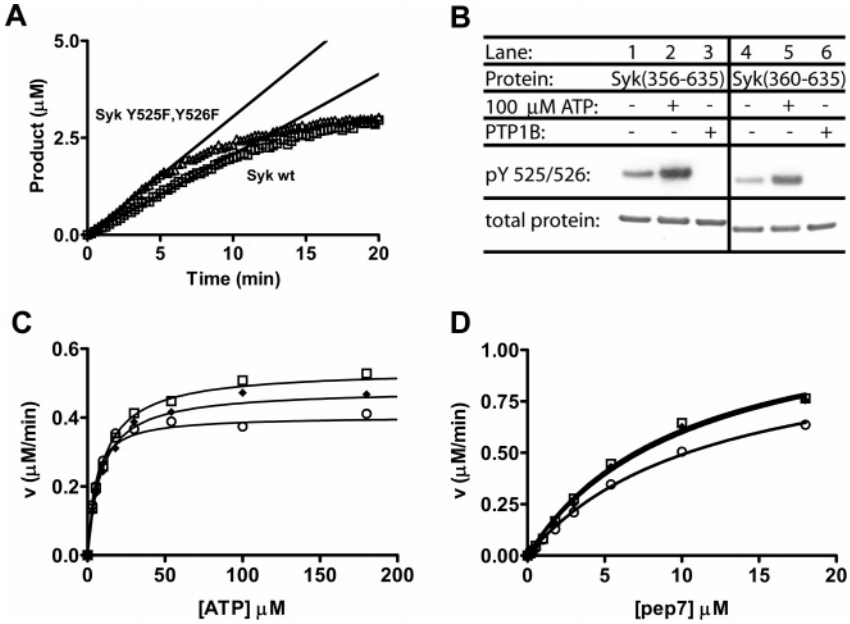

FIGURE 4: Role of activation loop phosphorylation in the activity of the Syk kinase domain. (A) Comparison of the activity of Syk(356−635) Y525F,Y526F with that of wild-type Syk(356−635). Shown is the time course of product formation as a function of time for both constructs at a concentration of 0.5 nM. The solid lines are the linear best fits to the initial phase of the reaction time courses (the first 5 min for both constructs) and provide velocities of 313 ± 4 and 217 ± 7 nM/min for Syk(356−635) Y525F,Y526F and wild-type Syk(356−635), respectively. (B) Western blot of Syk(356−635) and Syk(360−625) using a Tyr 525/Tyr 526 phosphospecific antibody. Syk(356−635) and Syk(360−635) were incubated with buffer, 100 μM Mg^{2+}/ATP, or PTP1B and probed for activation loop phosphorylation. The total protein loaded was ascertained from Coomassie staining of an equivalently loaded gel. (C and D) Activation loop phosphorylation of Syk(360−635) has little effect on Syk kinase domain activity. (C) Michaelis−Menten plot of v vs [ATP] for basal (◆), preincubated (□), and dephosphorylated (○) Syk. (D) Michaelis−Menten plot of v vs [pep 7] for basal (◆), preincubated (□), and dephosphorylated (○) Syk.

Table 2: Comparison of the Enzyme Parameters for Syk(360−635) and Full-Length Syk[a]

Syk form	K_m(ATP) (μM)[b]	K_m(pep 7) (μM)[b]	k_{cat} (min^{-1})[b]
Syk(360−635)	8.9 ± 5.2	10.9 ± 4.9	420 ± 120
Syk(360−635), pre-incubation	9.9 ± 4.4	10.0 ± 6.0	440 ± 160
Syk(360−635), dephosphorylation	4.6 ± 2.7	11.8 ± 6.9	368 ± 110
full-length Syk	33 ± 3	5.0 ± 0.4	38 ± 2

[a] Parameters were determined by fitting to the Michaelis−Menten equation (eq 1). [b] In these experiments, values of the kinetic constants were determined at a single concentration of the nonvaried substrate rather than by a global fitting procedure. Hence, these parameters will differ somewhat from parameters determined from a global analysis (see Experimental Procedures).

also varied. The measured reaction rates were then globally fit to models of competitive (eq 5), uncompetitive (eq 6), or mixed-type noncompetitive (eq 7) inhibition. YM193306 was found to be competitive with ATP and noncompetitive with S peptide (see Figure 5A,B). The K_i value for YM193306 was in the range of 5−20 nM depending on whether ATP or S peptide was varied (see Table 3), while the observed K_m values for ATP and S pep reproduce those determined from the two-substrate analysis described above. Data from these experiments are shown in double-reciprocal form in panels A and B of Figure 5 and Michaelis−Menten form in Figure 3A,B of the Supporting Information.

To further characterize the mechanism of substrate binding, the product of the reaction ADP was also used as an ATP-site inhibitor. The concentration of ADP was varied from 1 to 300 μM while simultaneously either ATP or S peptide was also varied. ADP, like YM193306, was found to be competitive with ATP and noncompetitive with S peptide (see Figure 5C,D). The K_i value for ADP was in the range of 30−70 μM depending on whether ATP or S peptide was varied (see Table 3); the observed K_m values for ATP and S pep were similar to those determined from the two-substrate analysis described above. The inhibition pattern demonstrated by both YM193306 and ADP indicates that S pep is not required to bind Syk before ATP (*30*).

To further characterize the mechanism of substrate binding, we sought inhibitors that would demonstrate competitive inhibition versus S peptide. The inhibitor potency of F peptide, an analogue of S peptide with phenylalanine replacing the catalytic tyrosine (see Figure 1B), was examined first. Surprisingly, F peptide did not inhibit Syk(360−635) at a concentration as high as 1.5 mM (Figure 6A). The inhibitory potency of tyrphostin AG538 was also explored. Tyrphostin AG538 has previously been demonstrated to have potency against the insulin-like growth factor 1 receptor tyrosine kinase (*34*). It also has a structure that suggests it might interact competitively with the substrate binding site of kinases (*35*; see Figure 1C) and was observed in preliminary experiments to have inhibitory potency against Syk(360−635) (data not shown). The K_i of tyrphostin AG538 for Syk was in the range of 10−20 μM (Table 3). However, tyrphostin AG538 did not exhibit competitive behavior versus S pep but rather demonstrated mixed, noncompetitive behavior against both ATP (Figure 6B) and S pep (Figure 6C). Hence, we failed to identify an inhibitor that binds competitively with S peptide.

The lack of an inhibitor that interacts exclusively with the substrate site of Syk precludes unambiguously ascertaining the order of substrate binding. The inhibitor binding data

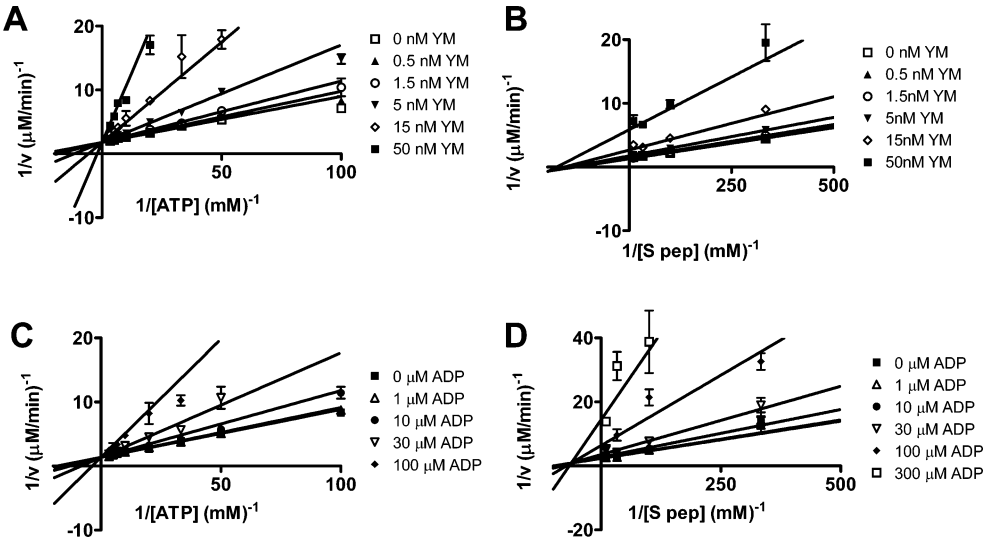

FIGURE 5: Inhibition of Syk with ATP analogues YM193306 and ADP monitored using radioactive capture. (A) Competitive inhibition of YM193306 with varied ATP. (B) Noncompetitive inhibition of YM193306 with varied S peptide. (C) Competitive inhibition of ADP with varied ATP. (D) Noncompetitive inhibition of ADP with varied S peptide. Shown in each case are double-reciprocal plots of $1/v$ vs either 1/[ATP] or 1/[S peptide] at varying inhibitor concentrations. Solid lines are representations of the nonlinear least-squares best fit of the entire data set. In panels A and C, the simulated lines are from the best fit parameters derived from a pure competitive model (eq 5). In panels B and D, the simulated lines are from the best fit parameters derived a mixed-type, noncompetitive model (eq 7). For best fit parameters, see Table 3. See Figure 3 of the Supporting Information for a representation of the full data sets in Michaelis−Menten form. Error bars are the standard deviations of multiple data points under each condition.

Table 3: Kinetic Constants for Syk Inhibition[a]

inhibitor	varied substrate	inhibitor pattern	V_{max} (μM/min)	K_m (μM)	K_{i1} (μM)	K_{i2} (μM)
YM193306	ATP	C[b]	0.56 ± 0.01	40 ± 2	0.0045 ± 0.0003	−
YM193306	S peptide	NC[c]	0.78 ± 0.02	7.6 ± 0.6	0.021 ± 0.009	0.014 ± 0.002
ADP	ATP	C[b]	0.74 ± 0.02	56 ± 4	31 ± 3	−
ADP	S peptide	NC[c]	0.43 ± 0.02	9.9 ± 1	32 ± 11	65 ± 36
tyrphostin AG538	ATP	NC[c]	0.54 ± 0.02	54 ± 8	10 ± 3	14 ± 2
tyrphostin AG538	S peptide	NC[c]	0.83 ± 0.09	20 ± 3	18 ± 5	9.6 ± 2

[a] Parameters are derived from the global, nonlinear best fit of the data to either a competitive (eq 5) or noncompetitive (eq 7) kinetic model. Uncertainties represent the standard error from the global fitting procedure. [b] Competitive. [c] Noncompetitive.

are therefore consistent with either a random order of binding (Figure 6D, left side of the panel) or an ordered binding with ATP binding first (Figure 6D, right side of the panel).

Comparison of Syk(360−635) to Full-Length Syk. The experiments described thus far have primarily been performed with Syk(360−635), a truncated form of Syk consisting of the isolated kinase domain. This form of the protein had the highest level of enzyme activity in a preliminary characterization of several different-length forms of the enzyme (data not shown). While Syk(360−635) is well-behaved for kinetic studies, it is conceivable that this enzyme form has properties that distinguish it from full-length Syk. To ascertain how closely Syk(360−635) mimicked full-length Syk, we obtained full-length Syk and characterized its kinetic properties using the real time fluorescence kinase assay.

We examined the phosphorylation state of full-length Syk using Western blotting with a phosphospecific antibody and found that, like Syk(360−635), full-length Syk is phosphorylated in its activation loop following purification (Figure 7A). Like Syk(360−635), full-length Syk also phosphorylates pep 7 in the fluorescence kinase assay; full-length Syk also shows activity in its basal state similar to that when it is preincubated with 100 μM ATP (Figure 7B). We next set out to demonstrate whether product formation was linear with time and enzyme concentration for full-length Syk studied in its purified state. As expected, the level of phosphorylated pep 7 did increase linearly with time at each enzyme concentration (Figure 7C), and the overall velocity of the reaction was also linear with enzyme concentration (Figure 7C inset). Varying the ATP concentration at a constant pep 7 concentration provided a K_m for ATP of 33 ± 3 μM (Figure 7D), while varying the pep 7 concentration at a constant ATP concentration provided a K_m for pep 7 of 5 ± 0.4 μM (Figure 7E) (the time courses of product formation for these experiments are shown in Figure 5A,B of the Supporting Information). The values are both within 4-fold of the K_m values for Syk(360−635) in its basal state (Table 2). However, the maximal activity for full-length Syk was observed to be more than 10-fold less than for Syk(360−635) (see Table 2). To confirm this difference in activity, the velocities of Syk(360−635) and full-length Syk were directly compared by examining the time course of pep 7 phosphorylation using an equivalent enzyme concentration of 1 nM (Figure 7F). It was revealed that the activity of Syk(360−635) (514 ± 4 nM/min) is indeed significantly greater than that of full-length Syk (32 ± 2 nM/min). The activity difference between Syk(360−635) and full-length Syk was observed with both the fluorescence and radioactive assays (see Figure 5C,D of the Supporting Information). Furthermore, similar enzyme activities were observed for different protein preparations of both full-length Syk (Figure 7B) and

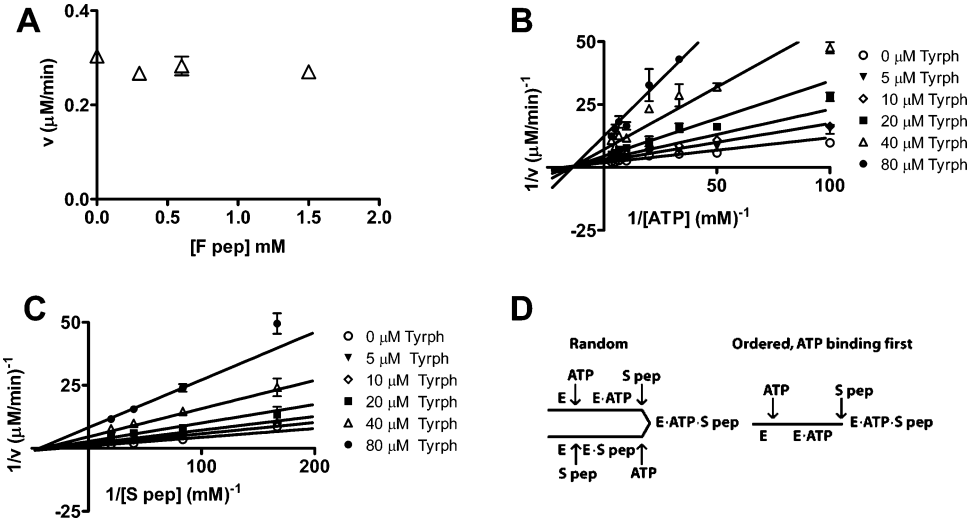

FIGURE 6: Inhibition of Syk with substrate analogues F peptide and tyrphostin AG538. (A) Lack of inhibition of Syk(360−635) with F peptide. Shown is the velocity vs F peptide concentration. (B) Noncompetitive inhibition of tyrphostin AG538 with both varied ATP and S peptide. Shown are double-reciprocal plots of $1/v$ vs 1/[ATP] (B) or 1/[S peptide] (C) at varying inhibitor concentrations. Solid lines are representations of the nonlinear least-squares best fit of the entire data set to a mixed-type, noncompetitive model (eq 7). For best fit parameters, see Table 3. See Figure 4 of the Supporting Information for a representation of the full data set in Michaelis−Menten form. Error bars are the standard deviations of multiple data points under each condition. (D) Kinetic inhibitor analysis indicates that the Syk kinetic mechanism is either random (left) or ordered with ATP binding first (right).

Syk kinase domain (data not shown), suggesting that differences in activity between full-length Syk and the Syk kinase domain are not particular to particular protein preparations. Hence, full-length Syk demonstrates reduced activity compared to Syk(360−635). This finding suggests that full-length Syk is autoinhibited by interactions outside the kinase domain.

DISCUSSION

Syk is a tyrosine kinase involved in signaling processes in B cells, mast cells, dendritic cells, and other immune cell types (*5*−*7*). The central role of Syk in immune cell activation makes it a potential target for treatment of rheumatoid arthritis, asthma, and allergies (*11*, *12*). Despite the significance of Syk to several disease processes, little to no characterization of the enzymology of Syk has yet been reported. In this work, we sought to better understand the kinetic mechanism and activation process of Syk. A new fluorescence kinase assay was employed that directly reports on Syk substrate phosphorylation in real time. Results from the fluorescence assay were directly compared to those from a more traditional radioactive kinase assay, and the two approaches were found to provide consistent information. Syk was found to employ a ternary complex (sequential-type) kinetic mechanism with little to no cooperativity between ATP and peptide substrate binding sites. The order of ATP and substrate binding to Syk is likely random, but an ordered mechanism with ATP binding first could not be completely ruled out due to the weak inhibition of substrate analogue inhibitors. Syk activity was not regulated by activation loop autophosphorylation since a Y525F,Y526F double mutant exhibited activity identical to that of the wild type. However, a truncated Syk version consisting of its isolated kinase domain, Syk(360−635), did demonstrate significantly greater activity than full-length Syk.

In this work, kinase substrates containing an unnatural, fluorescent amino acid, the Sox amino acid, adjacent to the site of phosphorylation were employed to monitor Syk kinase activity in real time (*28*, *29*). The Sox amino acid more strongly coordinates Mg^{2+} following phosphorylation, resulting in an increase in fluorescence (see Figure 2). Here, we demonstrate for the first time that the Sox-based assay has utility for characterizing the steady state kinetics of kinases. The Sox-based approach has numerous advantages over other approaches, including (1) a robust signal change, (2) flexibility in placing the Sox amino acid at various positions within the peptide sequence (permitting maintenance of essential kinase recognition motifs near the phosphorylated residue), and (3) the absence of any indirect or coupling reactions required to detect activity (*36*). In this work, the Sox-based assay greatly facilitated examination of the time course of Syk phosphorylation which was useful for concluding that Syk(360−635) is maximally active in the absence of activation loop phosphorylation.

The two-substrate kinetic analysis performed here (see Figure 3) indicates that Syk utilizes a ternary complex of enzyme, peptide substrate, and ATP in catalysis. The substrate analogue inhibitor studies (see Figures 5 and 6) are consistent with either a random order of binding of these substrates to Syk or an ordered binding mechanism with ATP binding first. On the basis of the lack of communication between the ATP and peptide binding sites observed in the two-substrate analysis (see Table 1), a random order of binding is the more likely of these two scenarios for Syk. A random order of substrate binding is most commonly observed for protein kinases. It has been observed, for instance, for Src (*37*), epidermal growth factor receptor (*38*), and more recently for JNK (*39*). Ordered binding has been observed with some kinases, including p38 mitogen-activated protein kinase (*40*, *41*).

The order of binding of substrates to Syk could not be unambiguously assigned because of the weak potency of the substrate analogue inhibitor F peptide. Specifically, Syk showed no inhibition by F peptide up to 1.5 mM (Figure

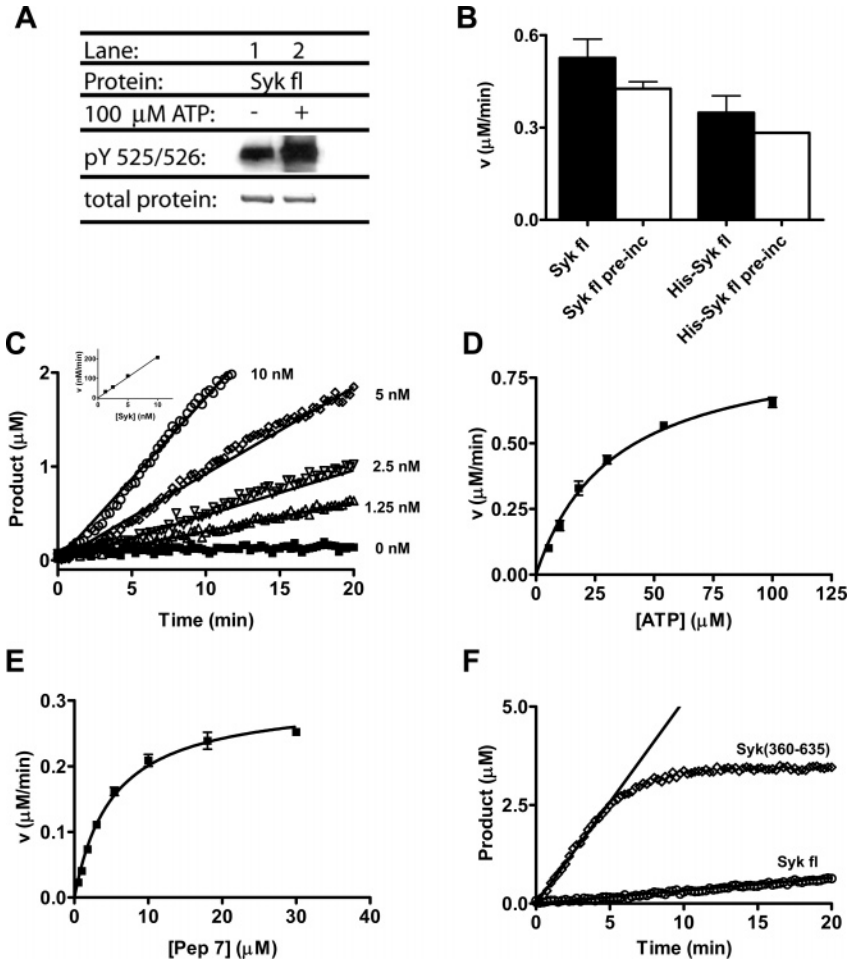

FIGURE 7: Mechanistic characterization of Syk fl using the real time fluorescence kinetic assay. (A) Western blot of the full-length protein using a Tyr 525/Tyr 526 phosphospecific antibody. Full-length Syk was incubated either with buffer or with 100 μM Mg^{2+}/ATP and probed for activation loop phosphorylation. The total protein loaded was ascertained from Coomassie staining of an equivalently loaded gel. (B) Comparison of the enzymatic activity for 10 nM full-length Syk that was (white bars) or was not (black bars) preincubated with Mg^{2+}/ATP prior to activity analysis. Two preparations of full-length Syk were tested: a GST-tagged preparation (left) and a His-tagged preparation (right). (C) Activity of Syk fl as a function of Syk fl concentration monitored by fluorescence using pep 7 as the substrate. Shown is the time course of product formation as a function of time at 0, 1.25, 2.5, 5, and 10 nM Syk fl. The solid lines are the linear best fits to the initial phase of the reaction time courses (10 min for all conditions). The inset shows the velocity values as a function of Syk fl concentration. The solid line is the linear best fit to the data, the slope of which provides a k_{cat} of 21 $\pm$ 0.4 min^{-1} under these conditions. (D) Michaelis−Menten plots demonstrate the K_m value for ATP of full-length Syk. Shown is the velocity of the reaction as a function of ATP concentration. The solid line is the best fit to the Michaelis−Menten equation and provides V_{max} and K_m values of 890 $\pm$ 4 nM/min and 33 $\pm$ 3 μM, respectively. Here, [Syk fl] = 20 nM and [pep 7] = 5 μM. (E) Michaelis−Menten plots demonstrate the K_m value for pep 7 of full-length Syk. Shown is the velocity of the reaction as a function of pep 7 concentration. The solid line is the best fit to the Michaelis−Menten equation and provides V_{max} and K_m values of 305 $\pm$ 8 nM/min and 5 $\pm$ 0.4 μM, respectively. Here, [Syk fl] = 10 nM and [ATP] = 25 μM. See Figure 5 of the Supporting Information for raw data. (F) Comparison of the activity of Syk(360−635) to that of full-length Syk. Shown is the time course of product formation as a function of time for either Syk(360−635) or full-length Syk, each at a concentration of 1 nM. The solid lines are the linear best fits to the initial phase of the reaction time courses [the first 5 min for both Syk(360−635) and full-length Syk] and provide velocities of 514 $\pm$ 4 and 32 $\pm$ 2 nM/min for Syk(360−635) and full-length Syk, respectively.

6A) even though the K_m value for the closely related S peptide substrate was 8.4 $\pm$ 2 μM (Table 1). The tyrosine kinases Csk and BTK are both similar to Syk in that the potency of substrate analogue inhibitors is much weaker than the K_m for substrate (*42*, *43*). For Csk, pre-steady state kinetic studies have uncovered a potential explanation for this behavior (*44*−*46*). Csk has been demonstrated to show a "substrate clamping" mechanism in which a fast phosphoryl transfer step compensates for a low substrate affinity, causing a low K_m value for substrate in comparison to the substrate K_d value. It is conceivable that Syk, like Csk, may also display some features of a substrate clamping mechanism, explaining the low potency of substrate analogue inhibitors with respect to the K_m value for the substrate peptide.

While Syk demonstrated steady state kinetic behavior similar to that of other tyrosine kinases such as BTK and Csk, the regulation of Syk by activation loop phosphorylation was atypical. In particular, many tyrosine kinases demonstrate an increase in activity following autophosphorylation within their activation loop (*47*−*49*); the reaction time course of these kinases typically display a lag phase in product formation due to the transition of the kinase from a low-activity to a high-activity state during the experiment (*43*, *50*). In this study, we monitored the time course of product formation by the Syk kinase domain and observed no lag phase in product formation, suggesting that the Syk kinase domain does not undergo an autophosphorylation-dependent increase in activity (Figure 3B). To further explore if Syk is

regulated by activation loop autophosphorylation, we also studied a Syk mutant in which the two activation loop tyrosines (Tyr 525 and Tyr 526) were mutated to phenylalanine. The Syk Y525F,Y526F mutant was found to have activity identical to that of wild-type Syk (Figure 4A). Furthermore, we directly compared the activity of the phosphorylated and unphosphorylated forms of the Syk kinase domain and observed no difference in activity. Together, these findings indicate that the activity of the Syk kinase domain is not increased by activation loop phosphorylation. A crystal structure of the Syk kinase domain supports our finding that activation loop phosphorylation is not required for high Syk activity (*51*). In this structure, the kinase adopts a conformation typical for the active state of kinases despite not being phosphorylated at Tyr 525 or Tyr 526. Hence, the Syk(360−635) construct characterized here is a good model for an active conformation of Syk.

To examine if full-length Syk demonstrated kinetic behavior identical to that of Syk(360−635), we obtained full-length Syk and characterized its kinetic constants. Full-length Syk was found to have K_m values for both substrates similar to those of Syk(360−635), but Syk(360−635) was greater than 10-fold more active than full-length Syk. Why might the Syk kinase domain alone be more active than full-length Syk? One possibility is that the SH2 domains and linker region in full-length Syk interact with the kinase domain in a manner that represses Syk kinase activity in its basal state. Indeed, the recently determined crystal structure of Zap-70 (a homologue of Syk) in its basal state supports a model in which Zap-70 is repressed in activity due to intramolecular interactions between the kinase domain and residues in the linker domain (*25*, *52*).

The finding here that the Syk kinase domain alone is significantly more active than full-length Syk provides further insight into understanding the mechanism of activation of full-length Syk. Within the cell, Syk is known to demonstrate increased activity following its recruitment to membrane receptors. The increase in activity may be part of a positive feedback loop that also includes the Src family kinase Lyn (*53*). Binding of Syk to ITAM motifs within cell surface receptors may also allosterically enhance Syk activity (*26*, *27*). Furthermore, Syk activity is also regulated by phosphorylation by other kinases (*24*). Despite many investigations regarding the activation of Syk, a clear picture of the molecular mechanism for how Syk makes the transition from its less active to more active conformation remains undefined. Future experiments that focus on dissecting the molecular mechanism of Syk activation would certainly provide a clearer picture of how Syk functions in signaling pathways and hence contribute to our understanding of the role of Syk in disorders associated with immune cells.

EXPERIMENTAL PROCEDURES

Protein Expression and Purification. Full-length and truncated versions of human Syk were cloned into a PVL 1392 vector for expression using baculovirus. Cloned versions of Syk include the full-length protein (residues 1−635), Syk(360−635), and Syk(356−635). The Syk(356−635) Y525F,Y526F mutant was constructed using the QuikChange mutagenesis kit (Stratagene, La Jolla, CA).

Each protein was expressed and purified in the same manner. For protein expression, Sf9 cells were infected at a multiplicity of infection of 0.5 at a density of 1.5×10^6 cells/mL. Cells were harvested 3 days following infection by centrifugation at 1000*g*. Cell pellets were resuspended in 250 mL of disruption buffer [50 mM Hepes (pH 7.5), 150 mM NaCl, 5% glycerol, 0.1% Ipegal, and 200 mM arginine]. Cells were disrupted on ice using two passes through a microfluidizer at 15 000 psi. Following disruption, material was centrifuged at 10000*g* and the supernatant was collected and filtered using a SuperCap Capsule. Material was then incubated for 3 h with a Ni Sepharose FF resin that had been pre-equilibrated in disruption buffer with 20 mM imidazole. Resin was collected at 1000*g* and then washed four times using disruption buffer. Bound proteins were eluted using 25 mL of elution buffer [25 mM Hepes (pH 7.6), 5% glycerol, 150 mM NaCl, 10 mM methionine, and 200 mM imidazole] and concentrated to 5 mg/mL total protein. Material was applied to a Superdex XK16/60 column that had been pre-equilibrated with 600 mL of 50 mM Hepes (pH 7.5), 150 mM NaCl, 5 mM DTT, and 10 mM methionine. Samples were run at 1 mL/min, and 1 min fractions were collected. Fractions were analyzed using an 8 to 16% Tris-glycine gel, pooled, and stored at −80 °C.

Using the procedure described above, a low yield of full-length His-tagged Syk was obtained due to the instability of the protein. Therefore, full-length Syk was acquired commercially from Invitrogen (Carlsbad, CA; catalog no. PV3857), and this version of the protein was used for most of the characterization of full-length Syk described here.

Syk Enzyme Assays. Syk enzyme activity was assessed using the increase in fluorescence of peptides containing the Sox amino acid. Pep 3, pep 5, and pep 7 were acquired from Invitrogen (catalog nos. KNZ3031, KNZ3051, and KNZ3071, respectively). Assays were performed in a buffer of 20 mM Hepes (pH 7.15), 0.1 mM EGTA, 0.1 mM DTT, 0.5 mg/mL BSA, and 10 mM $MgCl_2$ and were conducted in either 96-well or 384-well black plates (Corning Inc., Corning, NY) using a final assay volume of 50 or 20 μL, respectively. A SpectraMax GeminiXS fluorescence plate reader (Molecular Devices, Sunnyvale, CA) was used for data collection. The excitation wavelength was 360 nm, and the emission wavelength was 485 nm. Data were typically collected at 15 s intervals using two reads/well and a fluorescence cutoff of 455 nm. For assessment of the activity of the Syk Y525F,Y526F mutant, a Syk(356−635) construct was employed since the both the wild type and mutant construct were readily available.

Syk activity was also monitored using the incorporation of $^{33}PO_4$ from [^{33}P]ATP into a biotin-tagged peptide substrate. Using this approach, the peptide substrate was isolated from unreacted radioactive material using streptavidin-coated beads (Amersham Biosciences, Piscataway, NJ). The buffer for this enzyme assay was 25 mM Tris-HCl (pH 7.5), 25 mM glycerol 2-phosphate, 1 mM EGTA, 1 mM $NaVO_4$, 0.1% BSA, and 1 mM DTT. The sequence of the S peptide substrate (see Figure 1) was derived from HS1 protein and has previously been demonstrated to be a good substrate for Syk (*54*, *55*). Experiments were typically conducted for 15 min. At the end of the time course, assay plates were quenched, washed with 2 M NaCl with 1% phosphoric acid, dried, and subjected to scintillation counting. Other details of the radioactive enzyme assay have been described previously (*43*).

Western Blot Analysis. Western blots were performed with a Syk Tyr 525/526 phosphospecific antibody from Cell Signaling Technologies (Danvers, MA) used at a 1:500 dilution. Preincubation of Syk with Mg^{2+}/ATP was performed for 15 min at room temperature in a buffer of 20 mM Hepes (pH 7.15), 0.1 mM EGTA, 0.1 mM DTT, 0.5 mg/mL BSA, and 10 mM $MgCl_2$ at an ATP concentration of 100 μM. Dephosphorylation reactions were performed at room temperature for 1 h with PTP1B (Invitrogen) at a concentration of 2 μM. For kinase assays following incubation with PTP1B, 10 μM sodium vanadate was included in the buffer to inhibit phosphatase activity.

Time Course Analysis and K_m Evaluation. When a time course of Syk product formation was determined using the fluorescence assay, the assay contained 20 μM ATP and 5 μM pep 7. The velocity was evaluated from the initial phase of the reaction time course (typically the first 10−15 min). The signal change was converted to product formation (micromolar) using a solution provided by the manufacturer consisting of a phosphorylated version of pep 7.

To determine the K_m for ATP and pep 7 of Syk(360−635), ATP and peptide concentrations were varied from 1 to 180 μM and from 0.1 to 18.0 μM, respectively. To determine the K_m for ATP of full-length Syk, the ATP concentration was varied at quarter-log scale from 5.4 to 100 μM at a constant pep 7 concentration. Likewise, to determine the K_m for pep 7 of full-length Syk, the pep 7 concentration was varied at quarter-log scale from 0.54 to 30 μM at a constant ATP concentration. The nonvaried substrate concentrations were 20 μM for ATP and 5 μM for pep 7. The data were evaluated using the Michaelis−Menten equation to determine the K_m values and maximal velocity:

$$v = \frac{V_{max}[S]}{K_m + [S]} \quad (1)$$

where K_m is the Michaelis constant for one substrate at a constant concentration of the other substrate, k_{cat} is the maximal velocity at a particular value of nonvaried substrate, and [S] is the varied substrate concentration. Data analysis was conducted with GraphPad Prism 4.0 (GraphPad Software, Inc., San Diego, CA).

Two-Substrate Analysis with Syk. To perform the two-substrate analysis using the fluorescence assay, ATP and pep 7 were varied in a matrix at quarter-log intervals from 3.0 to 54 μM and from 1.8 to 30 μM, respectively. Likewise, the two-substrate analysis performed using the radioactive assay was performed by varying the ATP and S pep concentrations from 1 to 50 μM and from 6 to 150 μM, respectively. To assess the quality of the data, a preliminary analysis was performed that has previously been described (*43*).

Following the preliminary analysis, the complete set of velocity data was fit to expressions describing either a ternary complex or a ping-pong enzymatic mechanism. For the fluorescence data, the equation for a ternary complex mechanism is

$$v = \frac{V_{max}[ATP][pep\ 7]}{[ATP][pep\ 7] + [ATP]K_m^{pep\ 7} + [pep\ 7]K_m^{ATP} + K_m^{ATP}K_a^{pep\ 7}} \quad (2)$$

where K_m^{pep7} and K_m^{ATP} are Michaelis constants of pep 7 and ATP, respectively, and $K_a^{pep\ 7}$ is the association constant of pep 7 for Syk. Here the α factor, a measure of cooperativity between the ATP and pep 7 sites, is the ratio of the K_m values to dissociation constants:

$$\alpha = \frac{K_m^{pep\ 7}}{K_a^{pep\ 7}} = \frac{K_m^{ATP}}{K_a^{ATP}} \quad (3)$$

where K_a^{ATP} is the dissociation constant of ATP for Syk. The expression for the ping-pong enzymatic mechanism is given by

$$v = \frac{V_{max}[ATP][pep\ 7]}{[ATP][pep\ 7] + [ATP]K_m^{pep\ 7} + [pep\ 7]K_m^{ATP}} \quad (4)$$

To evaluate how well each model described the data, the value of the reduced sum of squares was examined. For Syk, the ternary complex model provided a significantly better fit than the ping-pong model.

Order of Substrate Binding. For experiments with substrate analogue inhibitors YM193306, ADP, F peptide, and tyrphostin AG538, the inhibitors were preincubated with Syk for 10−15 min before initiation of the enzyme reaction. Following preliminary analysis (*43*), data sets were fit to several different models to ascertain the mechanism of inhibition. These included a model of competitive inhibition

$$v = \frac{V_{max}[S]}{K_M(1 + [I]/K_{i1}) + [S]} \quad (5)$$

a model of uncompetitive inhibition

$$v = \frac{V_{max}[S]}{K_m + [S](1 + [I]/K_{i2})} \quad (6)$$

or a model of noncompetitive (mixed) inhibition

$$v = \frac{V_{max}[S]}{K_m(1 + [I]/K_{i1}) + [S](1 + [I]/K_{i2})} \quad (7)$$

In these equations, K_{i1} and K_{i2} are the inhibition constants for binding to the enzyme alone and the enzyme−peptide complex, respectively, and [I] is the inhibitor concentration. The quality of the fit of the data to each of the models was evaluated by examining the reduced sum of squares to ascertain the correct model for each data set.

ACKNOWLEDGMENT

We thank Wajiha Kahn and Waleed Danho for peptide synthesis, Emily Tsang for assistance with Western blotting, Jerome Deval and Mohammad Hekmat-Nejad for critical reading of the manuscript, and Ronald Hill, Tobias Gabriel, Yan Lou, and Andreas Kuglstatter for useful discussion.

SUPPORTING INFORMATION AVAILABLE

Time course data of Syk product formation and plots of enzyme velocity versus substrate concentration. This material

is available free of charge via the Internet at http://pubs.acs.org.

REFERENCES

1. Coopman, P. J., and Mueller, S. C. (2006) The Syk tyrosine kinase: A new negative regulator in tumor growth and progression, *Cancer Lett. 241*, 159−173.
2. Yanagi, S., Inatome, R., Takano, T., and Yamamura, H. (2001) Syk expression and novel function in a wide variety of tissues, *Biochem. Biophys. Res. Commun. 288*, 495−498.
3. Sada, K., Takano, T., Yanagi, S., and Yamamura, H. (2001) Structure and function of Syk protein-tyrosine kinase, *J. Biochem. 130*, 177−186.
4. Geahlen, R. L., and Burg, D. L. (1994) The role of Syk in cell signaling, *Adv. Exp. Med. Biol. 365*, 103−109.
5. Reth, M., and Wienands, J. (1997) Initiation and processing of signals from the B cell antigen receptor, *Annu. Rev. Immunol. 15*, 453−479.
6. Siraganian, R. P., Zhang, J., Suzuki, K., and Sada, K. (2002) Protein tyrosine kinase Syk in mast cell signaling, *Mol. Immunol. 38*, 1229−1233.
7. Berton, G., Mocsai, A., and Lowell, C. A. (2005) Src and Syk kinases: Key regulators of phagocytic cell activation, *Trends Immunol. 26*, 208−214.
8. Cheng, A. M., Rowley, B., Pao, W., Hayday, A., Bolen, J. B., and Pawson, T. (1995) Syk tyrosine kinase required for mouse viability and B-cell development, *Nature 378*, 303−306.
9. Costello, P. S., Turner, M., Walters, A. E., Cunningham, C. N., Bauer, P. H., Downward, J., and Tybulewicz, V. L. (1996) Critical role for the tyrosine kinase Syk in signalling through the high affinity IgE receptor of mast cells, *Oncogene 13*, 2595−2605.
10. Zhang, J., Berenstein, E. H., Evans, R. L., and Siraganian, R. P. (1996) Transfection of Syk protein tyrosine kinase reconstitutes high affinity IgE receptor-mediated degranulation in a Syk-negative variant of rat basophilic leukemia RBL-2H3 cells, *J. Exp. Med. 184*, 71−79.
11. Ulanova, M., Duta, F., Puttagunta, L., Schreiber, A. D., and Befus, A. D. (2005) Spleen tyrosine kinase (Syk) as a novel target for allergic asthma and rhinitis, *Expert Opin. Ther. Targets 9*, 901−921.
12. Wong, B. R., Grossbard, E. B., Payan, D. G., and Masuda, E. S. (2004) Targeting Syk as a treatment for allergic and autoimmune disorders, *Expert Opin. Invest. Drugs 13*, 743−762.
13. Hamerman, J. A., and Lanier, L. L. (2006) Inhibition of immune responses by ITAM-bearing receptors, *Sci STKE 2006*, re1.
14. Dal Porto, J. M., Gauld, S. B., Merrell, K. T., Mills, D., Pugh-Bernard, A. E., and Cambier, J. (2004) B cell antigen receptor signaling 101, *Mol. Immunol. 41*, 599−613.
15. Futterer, K., Wong, J., Grucza, R. A., Chan, A. C., and Waksman, G. (1998) Structural basis for Syk tyrosine kinase ubiquity in signal transduction pathways revealed by the crystal structure of its regulatory SH2 domains bound to a dually phosphorylated ITAM peptide, *J. Mol. Biol. 281*, 523−537.
16. Grucza, R. A., Futterer, K., Chan, A. C., and Waksman, G. (1999) Thermodynamic study of the binding of the tandem-SH2 domain of the Syk kinase to a dually phosphorylated ITAM peptide: Evidence for two conformers, *Biochemistry 38*, 5024−5033.
17. Kumaran, S., Grucza, R. A., and Waksman, G. (2003) The tandem Src homology 2 domain of the Syk kinase: A molecular device that adapts to interphosphotyrosine distances, *Proc. Natl. Acad. Sci. U.S.A. 100*, 14828−14833.
18. Lupher, M. L., Jr., Rao, N., Lill, N. L., Andoniou, C. E., Miyake, S., Clark, E. A., Druker, B., and Band, H. (1998) Cbl-mediated negative regulation of the Syk tyrosine kinase. A critical role for Cbl phosphotyrosine-binding domain binding to Syk phosphotyrosine 323, *J. Biol. Chem. 273*, 35273−35281.
19. Hong, J. J., Yankee, T. M., Harrison, M. L., and Geahlen, R. L. (2002) Regulation of signaling in B cells through the phosphorylation of Syk on linker region tyrosines. A mechanism for negative signaling by the Lyn tyrosine kinase, *J. Biol. Chem. 277*, 31703−31714.
20. Moon, K. D., Post, C. B., Durden, D. L., Zhou, Q., De, P., Harrison, M. L., and Geahlen, R. L. (2005) Molecular basis for a direct interaction between the Syk protein-tyrosine kinase and phosphoinositide 3-kinase, *J. Biol. Chem. 280*, 1543−1551.
21. Latour, S., Zhang, J., Siraganian, R. P., and Veillette, A. (1998) A unique insert in the linker domain of Syk is necessary for its function in immunoreceptor signaling, *EMBO J. 17*, 2584−2595.
22. Chu, D. H., Morita, C. T., and Weiss, A. (1998) The Syk family of protein tyrosine kinases in T-cell activation and development, *Immunol. Rev. 165*, 167−180.
23. Zhang, J., Kimura, T., and Siraganian, R. P. (1998) Mutations in the activation loop tyrosines of protein tyrosine kinase Syk abrogate intracellular signaling but not kinase activity, *J. Immunol. 161*, 4366−4374.
24. Zhang, J., Billingsley, M. L., Kincaid, R. L., and Siraganian, R. P. (2000) Phosphorylation of Syk activation loop tyrosines is essential for Syk function. An in vivo study using a specific anti-Syk activation loop phosphotyrosine antibody, *J. Biol. Chem. 275*, 35442−35447.
25. Brdicka, T., Kadlecek, T. A., Roose, J. P., Pastuszak, A. W., and Weiss, A. (2005) Intramolecular regulatory switch in ZAP-70: Analogy with receptor tyrosine kinases, *Mol. Cell. Biol. 25*, 4924−4933.
26. Shiue, L., Zoller, M. J., and Brugge, J. S. (1995) Syk is activated by phosphotyrosine-containing peptides representing the tyrosine-based activation motifs of the high affinity receptor for IgE, *J. Biol. Chem. 270*, 10498−10502.
27. Rowley, R. B., Burkhardt, A. L., Chao, H. G., Matsueda, G. R., and Bolen, J. B. (1995) Syk protein-tyrosine kinase is regulated by tyrosine-phosphorylated Igα/Igβ immunoreceptor tyrosine activation motif binding and autophosphorylation, *J. Biol. Chem. 270*, 11590−11594.
28. Shults, M. D., Janes, K. A., Lauffenburger, D. A., and Imperiali, B. (2005) A multiplexed homogeneous fluorescence-based assay for protein kinase activity in cell lysates, *Nat. Methods 2*, 277−283.
29. Shults, M. D., Carrico-Moniz, D., and Imperiali, B. (2006) Optimal Sox-based fluorescent chemosensor design for serine/threonine protein kinases, *Anal. Biochem. 352*, 198−207.
30. Copeland, R. A. (2005) *Evaluation of Enzyme Inhibitors in Drug Discovery*, John Wiley and Sons, Hoboken, NJ.
31. Segel, I. H. (1975) *Enzyme Kinetics*, John Wiley and Sons, Hoboken, NJ.
32. Hisamichi, H., Naito, R., Toyoshima, A., Kawano, N., Ichikawa, A., Orita, A., Orita, M., Hamada, N., Takeuchi, M., Ohta, M., and Tsukamoto, S. (2005) Synthetic studies on novel Syk inhibitors. Part 1: Synthesis and structure-activity relationships of pyrimidine-5-carboxamide derivatives, *Bioorg. Med. Chem. 13*, 4936−4951.
33. Wilkinson, S. E., and Harris, W. (2000) Selective Tyrosine Kinase Inhibitors, *Emerging Drugs 287*, 287−297.
34. Blum, G., Gazit, A., and Levitzki, A. (2000) Substrate competitive inhibitors of IGF-1 receptor kinase, *Biochemistry 39*, 15705−15712.
35. Levitzki, A., and Mishani, E. (2006) Tyrphostins and other tyrosine kinase inhibitors, *Annu. Rev. Biochem. 75*, 93−109.
36. Rothman, D. M., Shults, M. D., and Imperiali, B. (2005) Chemical approaches for investigating phosphorylation in signal transduction networks, *Trends Cell Biol. 15*, 502−510.
37. Boerner, R. J., Barker, S. C., and Knight, W. B. (1995) Kinetic mechanisms of the forward and reverse pp60c-src tyrosine kinase reactions, *Biochemistry 34*, 16419−16423.
38. Posner, I., Engel, M., and Levitzki, A. (1992) Kinetic model of the epidermal growth factor (EGF) receptor tyrosine kinase and a possible mechanism of its activation by EGF, *J. Biol. Chem. 267*, 20638−20647.
39. Niu, L., Chang, K. C., Wilson, S., Tran, P., Zuo, F., and Swinney, D. C. (2007) Kinetic characterization of human JNK2α2 reaction mechanism using substrate competitive inhibitors, *Biochemistry 46*, 4775−4784.
40. LoGrasso, P. V., Frantz, B., Rolando, A. M., O'Keefe, S. J., Hermes, J. D., and O'Neill, E. A. (1997) Kinetic mechanism for p38 MAP kinase, *Biochemistry 36*, 10422−10427.
41. Chen, G., Porter, M. D., Bristol, J. R., Fitzgibbon, M. J., and Pazhanisamy, S. (2000) Kinetic mechanism of the p38-α MAP kinase: Phosphoryl transfer to synthetic peptides, *Biochemistry 39*, 2079−2087.
42. Cole, P. A., Burn, P., Takacs, B., and Walsh, C. T. (1994) Evaluation of the catalytic mechanism of recombinant human Csk (C-terminal Src kinase) using nucleotide analogs and viscosity effects, *J. Biol. Chem. 269*, 30880−30887.
43. Dinh, M., Grunberger, D., Ho, H., Tsing, S. Y., Shaw, D., Lee, S., Barnett, J., Hill, R. J., Swinney, D. C., and Bradshaw, J. M.

(2007) Activation mechanism and steady state kinetics of Bruton's tyrosine kinase, *J. Biol. Chem. 282*, 8768−8776.
44. Lieser, S. A., Aubol, B. E., Wong, L., Jennings, P. A., and Adams, J. A. (2005) Coupling phosphoryl transfer and substrate interactions in protein kinases, *Biochim. Biophys. Acta 1754*, 191−199.
45. Lieser, S. A., Shindler, C., Aubol, B. E., Lee, S., Sun, G., and Adams, J. A. (2005) Phosphoryl transfer step in the C-terminal Src kinase controls Src recognition, *J. Biol. Chem. 280*, 7769−7776.
46. Lieser, S. A., Shaffer, J., and Adams, J. A. (2006) SRC tail phosphorylation is limited by structural changes in the regulatory tyrosine kinase Csk, *J. Biol. Chem. 281*, 38004−38012.
47. Johnson, L. N., Noble, M. E., and Owen, D. J. (1996) Active and inactive protein kinases: Structural basis for regulation, *Cell 85*, 149−158.
48. Huse, M., and Kuriyan, J. (2002) The conformational plasticity of protein kinases, *Cell 109*, 275−282.
49. Adams, J. A. (2003) Activation loop phosphorylation and catalysis in protein kinases: Is there functional evidence for the autoinhibitor model? *Biochemistry 42*, 601−607.
50. Moarefi, I., LaFevre-Bernt, M., Sicheri, F., Huse, M., Lee, C. H., Kuriyan, J., and Miller, W. T. (1997) Activation of the Src-family tyrosine kinase Hck by SH3 domain displacement, *Nature 385*, 650−653.
51. Atwell, S., Adams, J. M., Badger, J., Buchanan, M. D., Feil, I. K., Froning, K. J., Gao, X., Hendle, J., Keegan, K., Leon, B. C., Muller-Dieckmann, H. J., Nienaber, V. L., Noland, B. W., Post, K., Rajashankar, K. R., Ramos, A., Russell, M., Burley, S. K., and Buchanan, S. G. (2004) A novel mode of Gleevec binding is revealed by the structure of spleen tyrosine kinase, *J. Biol. Chem. 279*, 55827−55832.
52. Deindl, S., Kadlecek, T. A., Brdicka, T., Cao, X., Weiss, A., and Kuriyan, J. (2007) Structural basis for the inhibition of tyrosine kinase activity of ZAP-70, *Cell 129*, 735−746.
53. Rolli, V., Gallwitz, M., Wossning, T., Flemming, A., Schamel, W. W., Zurn, C., and Reth, M. (2002) Amplification of B cell antigen receptor signaling by a Syk/ITAM positive feedback loop, *Mol. Cell 10*, 1057−1069.
54. Schmitz, R., Baumann, G., and Gram, H. (1996) Catalytic specificity of phosphotyrosine kinases Blk, Lyn, c-Src, and Syk assessed by phage display, *J. Mol. Biol. 260*, 664−677.
55. Baldock, D., Graham, B., Akhlaq, M., Graff, P., Jones, C. E., and Menear, K. (2000) Purification and characterization of human Syk produced using a baculovirus expression system, *Protein Expression Purif. 18*, 86−94.

BI701596U